Behavior recognition and fuel consumption prediction of tractor sowing operations using smartphone

Lili Yang[1,2], Weize Tian[1,2], Weixin Zhai[1,2], Xinxin Wang[1,2], Zhibo Chen[1,2], Long Wen[1,2], Yuanyuan Xu[1,2], Caicong Wu[1,2*]

(1. *College of Information and Electrical Engineering, China Agricultural University, Beijing 100083, China*;
2. *Key Laboratory of Agricultural Machinery Monitoring and Big Data Application, Ministry of Agriculture and Rural Affairs, Beijing 100083, China*)

Abstract: In order to qualitatively recognize the behaviors and investigate the relationship between fuel consumption and machinery driving modes of the tractor in a low-cost approach, this study proposed a method for behavior recognition and fuel consumption prediction of tractor sowing operations using a smartphone. First, three driving modes were developed for maize sowing scenarios: manual driving assisted driving and unmanned driving. While sowing, smartphone software and CAN (Controller Area Network) storage devices collected both positional data and engine operating conditions. Second, the tractor trajectory points were divided into kinematic sequences, with six driving cycle indicators built in each series based on the time window. Based on the semantic information of the kinematic sequences, the three operations of sowing, seeds filling, and turning round were well recognized. Last, a model for maize sowing fuel consumption forecast was advanced using the principal component analyses and random forest algorithm, regarding three factors: driving cycles, operating behaviors, and driving patterns. When compared to the traditional *K*-means algorithm, the results demonstrated that the harmonic mean of the precision and recall (F1 score) of sowing behavior recognition, seeds filling behavior recognition, and turning behavior recognition were enhanced by 2.06%, 8.99%, and 21.79%, respectively. In terms of the impacts of driving modes and operating behaviors on fuel consumption, assisted driving mode had the lowest fuel usage for both sowing and turning behavior. Therefore, assisted driving is the most fuel-efficient mode for maize sowing. Combining the three driving modes, the relative error of the fuel consumption prediction model was 0.11 L/h, with the manual driving mode having the lowest relative error at 0.09 L/h. This research method lays the foundation for the optimization of tractor operation behavior, the selection of tractor driving mode, and the fine management of tractor fuel consumption.

Keywords: smartphone, kinematic sequence, operating behavior, fuel consumption forecast, tractor
DOI: 10.25165/j.ijabe.20221504.7454

Citation: Yang L L, Tian W Z, Zhai W X, Wang X X, Chen Z B, Wen L, et al. Behavior recognition and fuel consumption prediction of tractor sowing operations using a smartphone. Int J Agric & Biol Eng, 2022; 15(4): 154–162.

1 Introduction

In recent years, the level of agricultural mechanization in the country has steadily increased, resulting in an increase in agricultural fuel consumption[1]. The research on tractor fuel consumption has significant practical implications for rural environmental governance and the reduction of farmer capital investment[2].

Numerous research on the fuel usage of road cars is being conducted at the moment. Historically, the majority of classic fuel consumption models were constructed using vehicle dynamics principles. The comprehensive emission model (CMEM) uses engine running state characteristics to calculate fuel usage per second[3]. Complex parameters and inefficient computation were two of the model's less admirable aspects, along with an accurate representation of the physical meaning of the vehicle. In recent years, data-driven machine algorithms have been extensively applied in fuel consumption modeling. A portion of the models is based on vehicle driving cycle data. Built a panel data fixed-effect regression fuel consumption model based on the microscopic operating data, such as instantaneous speed and instantaneous fuel consumption of 199 large trucks in Beijing, and quantified the fuel-saving potential associated with improving five types of bad driving behaviors[4]. The parts of the models are based on the external environment when the vehicle is in motion. Established an oil consumption prediction model of open-pit mine vehicles based on particle swarm optimization and genetic algorithm based support vector machine (PSOGA-SVM), which related to the weather, road height difference, road condition, and other external environmental data of open-pit mine vehicle transportation[5]. Both vehicle driving conditions and the external environment are taken into consideration in some models. According to instantaneous driving conditions, slope, and ambient temperature, Constructed a microscopic fuel consumption

Receieved date: 2022-02-24 **Accepted date:** 2022-06-23
Biographies: **Lili Yang**, PhD, Associate Professor, research interests: big data mining of agricultural machinery, Email: llyang@cau.edu.cn; **Weize Tian**, MS, research interests: big data mining of agricultural machinery, Email: 15230173972@163.com; **Weixin Zhai**, PhD, Associate Professor, research interests: big data mining of agricultural machinery, Email: zhaiweixin@cau.edu.cn; **Xinxin Wang**, MS, research interests: big data mining of agricultural machinery, Email: 939994970@qq.com; **Zhibo Chen**, PhD, research interests: big data mining of agricultural machinery, Email: chenzb@cau.edu.cn; **Long Wen**, MS, research interests: Big data mining of agricultural machinery, Email: wl@cau.edu.cn; **Yuanyuan Xu**, MS, research interests: big data mining of agricultural machinery, Email: s20203081484@cau.edu.cn.

***Corresponding author: Caicong Wu**, PhD, Professor, research interests: big data mining of agricultural machinery, and driverless and cooperative operation. College of Information and Electrical Engineering, China Agricultural University, Beijing 100083, China. Tel: +86-13810521813, Email: wucc@cau.edu.cn.

prediction model for hybrid-electric buses based on Artificial Neural Network (ANN) and divided the instantaneous data into groups by the equal time to construct the mesoscopic fuel consumption prediction model based on ANN[6]. Building a truck fuel consumption prediction model based on random forest, support vector machine, and neural network by using the data of truck speed, weight, and the slope of the highway[7]. A linear mixed-effect model was constructed, which explored the impact of external environments on taxi drivers' safe driving and vehicle fuel consumption[8]. The model took into account vehicle driving cycle, road structure, and weather.

In summary, fuel consumption prediction for urban road vehicles is primarily based on two components of the vehicle driving cycle and the external environment. However, the tractor differs significantly from urban road vehicles in two respects. First, in most cases, the tractor has been operating at low speeds and under large loads; second, the working environment involves generally high temperature, high dust, and high vibration[9]. Data collection equipment that collects data in real-time OBD is commonly employed in the study of urban road car fuel consumption. However, in order to collect data for tractor fuel consumption study, aspects such as the equipment install ability, cost, and driver willingness must be considered. Mobile phone applications continue to diversify as smartphones gain popularity and mobile phone sensor technology advances. Numerous studies on on-road vehicle driving cycle modeling have been published, combining vehicle data obtained from mobile phone sensors with machine learning or deep learning algorithms, and these studies have contributed to the advancement of vehicle fuel consumption evaluation[10-12].

The research object of this work was agricultural tractors. It investigated the behavior recognition of operations behaviors in three driving modes based on the positioning data of smartphones. On top of this foundation, the relationship among tractor driving cycle, operating behavior, driving mode, and sowing fuel consumption was modeled using principal component analysis and random forest algorithm. A method for predicting tractor fuel consumption using a smartphone was proposed, which provides a reference for fuel consumption evaluation and supervision of tractors.

2 Materials and methods

2.1 Data collection

Experiments were carried out on Dongfeng 2204CVT wire-controlled tractor at Henanzhai town, Miyun District, Beijing city in May 2021. The tractor rated power 162 kW, rated speed 2200 r/min, rated pulling force 49 kN, displacement 8.8 L. Three driving modes were designed for maize sowing scenarios: manual driving, assisted driving, and unmanned driving. A schematic diagram of sowing in various driving modes is shown in Figure 1. The planting area of each mode is around 6.67 hm^2. The farmland is divided into strip areas and turning areas.

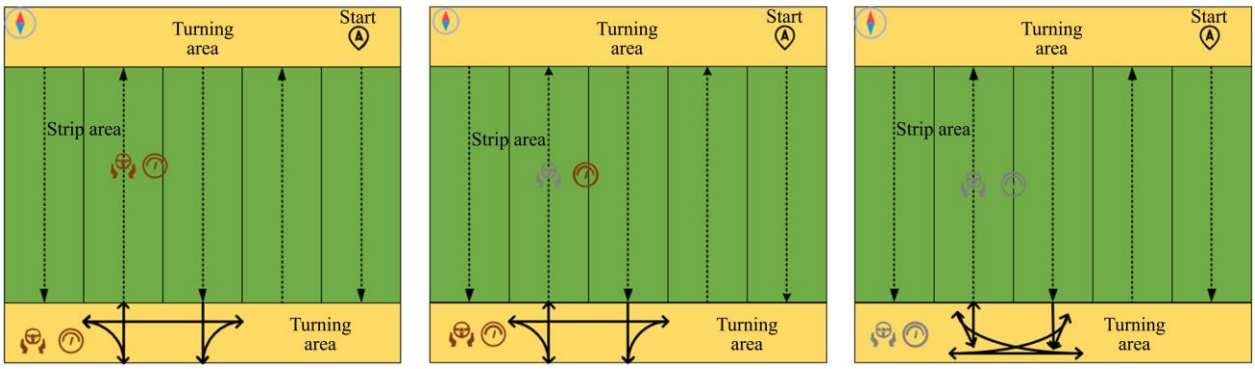

a. Manual driving mode b. Assisted driving mode c. Unmanned driving mode

Note: The steering wheel represents the direction control the gauge represents the speed control; gray represents the computer program control; brown represents the manual control. The dotted line in the strip area represents the agricultural machinery operation line, and the solid line represents the strip boundary.

Figure 1 Schematic diagram of sowing in three driving modes

A meter-level precision Huawei nova4 smartphone and a centimeter-level precision T100 vehicle-mounted terminal are placed in the cab for the data collection, which records tractor positioning data, including time, longitude, latitude, speed, etc. Table 1 reports the equipment characteristics. Simultaneously, the GCAN-401 storage instrument collects the tractor's instantaneous fuel consumption, speed, torque, and other engine operating variables. GCAN-401 can record data in a tractor CAN bus. It is 102 mm long, 63 mm wide, and 23 mm high, and the power supply voltage is 9-30 V. Three devices operate at the same frequency of 10 Hz.

The tractor operates in the way of shuttle sowing and fishtail turning mode, and detailed instructions are listed in Table 2. In manual driving mode, direction, and speed are controlled manually whether in strip areas or turning areas. In assisted driving mode, the direction was controlled by the computer program, and speed was controlled manually in strip areas, but direction and speed are manually controlled in turning areas. In unmanned driving mode, direction and speed were controlled by the computer program both in strip areas and turning areas.

Table 1 Huawei nova4 smartphone and T100 vehicle-mounted terminal characteristics

Equipment	Characteristic	Value
Huawei nova4 smartphone	Operating system	Android9.0
	Screen size/mm	162.54
	Battery capacity/mAh	3750
	ROM capacity/GB	128
	Positioning signal	Beidou, GPS, A-GPS, GLONASS
	Positioning precision	Meter-level
T100 vehicle-mounted terminal	Operating system	Android 6.0
	Screen size/mm	256.54
	Power consumption/W	≤12.0
	ROM capacity/GB	16
	Positioning signal	Beidou
	Positioning precision	Centimeter-level

Table 2 Operating instructions for the three driving modes

Mode	Strip area		Turning area	
	Speed	Direction	Speed	Direction
Manual driving mode				
Assisted driving mode				
Unmanned driving mode				

Note: The steering wheel represents the direction control the gauge represents the speed control; gray represents the computer program control; brown represents the manual control.

A total of 237 440 pieces of positional data and 237 510 pieces of engine operating condition data were collected. The Transverse Mercator Projection was employed to transform the positioning data from the WGS84 geodetic coordinate, to plane coordinates. The tractor engine operating condition data collected by the GCAN-401 storage instrument are all in a hexadecimal system. In order to facilitate the calculation, according to the conversion method in "Weichai Power Autonomous ECU Vehicle Network Communication Technology Application Specification", the hexadecimal data was converted into decimal. Due to the instability of smartphone hardware sensors and the vibration of the tractor, there were vacancies and various noises in positioning data[13]. The interpolation approach was used to fill in the missing values in the positioning data, resulting in the completion of 237 510 pieces of positioning data. The Kalman filter method was used to filter and denoise the speed data. According to the timestamp, the positioning data was matched with the fuel consumption data. Thus, the tractor's fuel consumption in different positions can be determined.

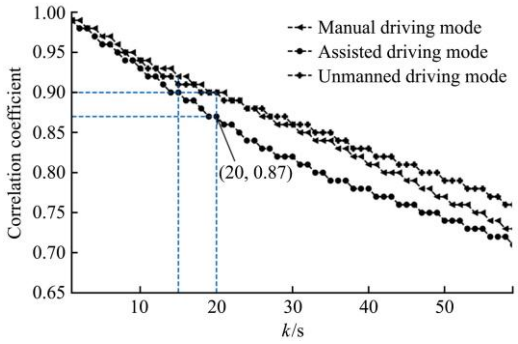

Note: v_t is the working speed of the tractor at the tth second, m/s; v_{t+k} is the working speed of the tractor at the $t+k$ second, m/s.

Figure 2 Tractor sowing operation v_t and v_{t+k} correlation

2.2 Kinematic sequence division and reliability examination of data collected via smartphone

2.2.1 Kinematic sequence division

Since a single instantaneous positioning data cannot reasonably reflect the behavioral characteristics of tractor operations. In this study, the continuous trajectory points of agricultural machinery operations were divided into multiple kinematic sequences according to a fixed time step. If the time of the kinematics sequence is too long, it may increase the probability that the trajectory points corresponding to different operation behaviors are divided into the same kinematics sequence. If the kinematic sequence time is too short, it will affect the calculation of working parameters such as idle speed and constant speed.

Different operating behaviors of agricultural machinery often correspond to different operating speeds[14]. Analysis of the correlation between the speed v_t in the t second and the speed v_{t+k} in the $t+k$ second when the tractor is in the three driving modes of the maize sowing. The value of k is 1-59 s. Correlation evaluation was carried out using Pearson's correlation coefficient. The correlation result between v_t and v_{t+k} is shown in Figure 2. The correlation between v_t and v_{t+k} is negatively correlated with k. When k is 15 s, the correlation coefficients under the three driving modes are 0.92, 0.90, and 0.91, which are all greater than 0.9, showing a strong correlation ($p<0.01$)[15]. When k is 20 s, the correlation coefficients in the three driving modes are 0.90, 0.87, and 0.90, respectively, which are slightly lower than when k is 15 s, but the correlation coefficients in both manual and unmanned driving modes are still greater than 0.9. When i is greater than 20, the correlation coefficients of the three driving modes are all less than 0.9, and the correlation gradually weakens. In order to ensure that the kinematic segments in the three driving modes have the same duration and high-speed correlation while keeping as many trajectory points as possible, the time step of each kinematic sequence is set to 20 s in this study. To verify the integrity of the trajectory data, a small amount of positioning data that does not meet the 20 s time step is also classified as a kinematics sequence. Each kinematics segment comprises additional semantic information such as average speed, acceleration time ratio, deceleration time ratio, etc. The experimental data of the three driving modes are divided into 1139 kinematic sequences.

This article makes the following provisions for tractor kinematic sequences' driving cycle referred to the stated standard of heavy vehicle driving cycle[16]:

1) The tractor is in an acceleration condition when the acceleration exceeds 0.15 m/s^2;

2) The tractor is in a decelerating condition when the acceleration is less than −0.15 m/s^2;

3) The tractor is in a constant speed working condition when the acceleration is greater than −0.15 m/s^2 and less than 0.15 m/s^2, and the speed is greater than or equal to 0.5 m/s;

4) The tractor is in an idling condition when the acceleration is greater than −0.15 m/s^2 and less than 0.15 m/s^2, and the speed is less than 0.5 m/s.

Fuel consumption is affected by a significant number of driving cycles[17]. The tractor driving cycle feature matrix $\boldsymbol{A}$ is constructed by estimating six driving cycles using the positioning data acquired by the smartphone. The six parameters of each kinematic sequence are the value of the average working speed of the tractor ($\bar{V}$), speed standard deviation (V_{std}), acceleration time ratio (P_a+), deceleration time ratio (P_a–), uniform time ratio ($P_{\bar{V}}$), idle time ratio (P_C).

2.2.2 Reliability examination of data collected via smartphone

The low-cost smartphone is more easily promoted than the high-priced centimeter-level positioning device. The feature matrices $\boldsymbol{A}'$ and $\boldsymbol{A}''$ of the tractor driving cycle are generated from smartphone data and centimeter-level data, respectively, to demonstrate the feasibility of recognizing the sowing behavior of the tractor based on smartphone data. Correlations between each dimension and the matrix $\boldsymbol{A}'$ and the matrix $\boldsymbol{A}''$ are evaluated, and the T2 distribution test is performed for each dimension. The results are summarized in Table 3.

By consulting the quantile table of the T distribution, when the number of samples is greater than 120, the absolute value of t in the T value distribution test is less than 1.96, proving that there is no significant difference in the driving cycle perceived by mobile devices or centimeter-level positioning devices[19]. Therefore, it is practicable to use smartphone positioning data to identify tractor behavior and predict fuel consumption.

Table 3 Correlation and distribution test of vehicle driving cycle based on smartphone and centimeter-level positioning equipment

Driving cycle	Pearson correlation coefficient	*T* value
Average speed	0.99**	1.19*
Speed standard deviation	0.91**	0.67*
Acceleration time ratio	0.61**	0.68*
Deceleration time ratio	0.78**	1.17*
Uniform time ratio	0.98**	1.72*
Idle time ratio	0.99**	−1.94*

Note: ** represents obvious in 0.01; * represents obvious in 0.05; Table 3 shows that the correlation coefficient of the driving cycle index between smartphone-based data and centimeter-level data is greater than 0.6, indicating that the two are highly correlated (p<0.01)[18].

2.3 Data analysis

2.3.1 Tractor sowing behavior recognition

To evaluate and assess the difference between tractor sowing behavior and fuel consumption, it is necessary to identify the operation behavior under three driving modes. Within a single kinematic sequence, the trajectory features and behavior are comparable. The segmentation of the kinematic sequence not only compresses the amount of data and reduces the running time of the clustering algorithm, but also generates additional kinds of driving condition indicators, endowing the trajectory within the segment with richer semantics. The clustering algorithm can learn more features, which improves the clustering result. Used the DBSCAN algorithm to distinguish between two types of agricultural machinery behaviors in the field and on the road, based on the speed and direction of the agricultural machinery, but the time complexity of the algorithm is high[20]. Therefore, this paper uses the *K*-means algorithm to perform preliminary clustering identification of motion sequences, as depicted in Figures 3a-3c.

The kinematic sequence can be classified into three categories using *K*-means analysis. The green dotted line corresponds to Category 1, which is concentrated in the strip areas and correlates to tractor sowing behavior. The blue dotted line represents Category 2, which is concentrated in the field head and correlates to the tractor seeds filling behavior. The yellow dotted line represents Category 3, which is concentrated at both ends of the field and corresponds to tractor turning behavior. Three labels are assigned to categories 1, 2, and 3. Because the manual driving speed is faster than assisted and unmanned driving, the green dotted lines in Figure 3a are straighter than those in Figure 3b and Figure 3c. Low speed can result in denser and more discrete trajectory point data collecting. Table 4 shows the recognition error rates calculated by the *K*-means method. Turning actions are incorrectly recognized as seeds filling behaviors in 81.51% of the clips. The primary reason for this is that the seeds filling behavior are frequently comparable to the turning behavior, in terms of the inescapable pause and huge idle time proportion. Therefore, it is necessary to further correct the initial kinematic sequence recognition findings after *K*-means clustering. As shown in Figure 4, this study proposed a technical route for operation behavior recognition based on the semantic information of kinematic sequence.

Table 4 *K*-means algorithm recognition error rates (%)

Category No.	Category 1	Category 2	Category 3
Category 1	--	5.88	5.88
Category 2	0.00	--	0.84
Category 3	5.88	81.51	--

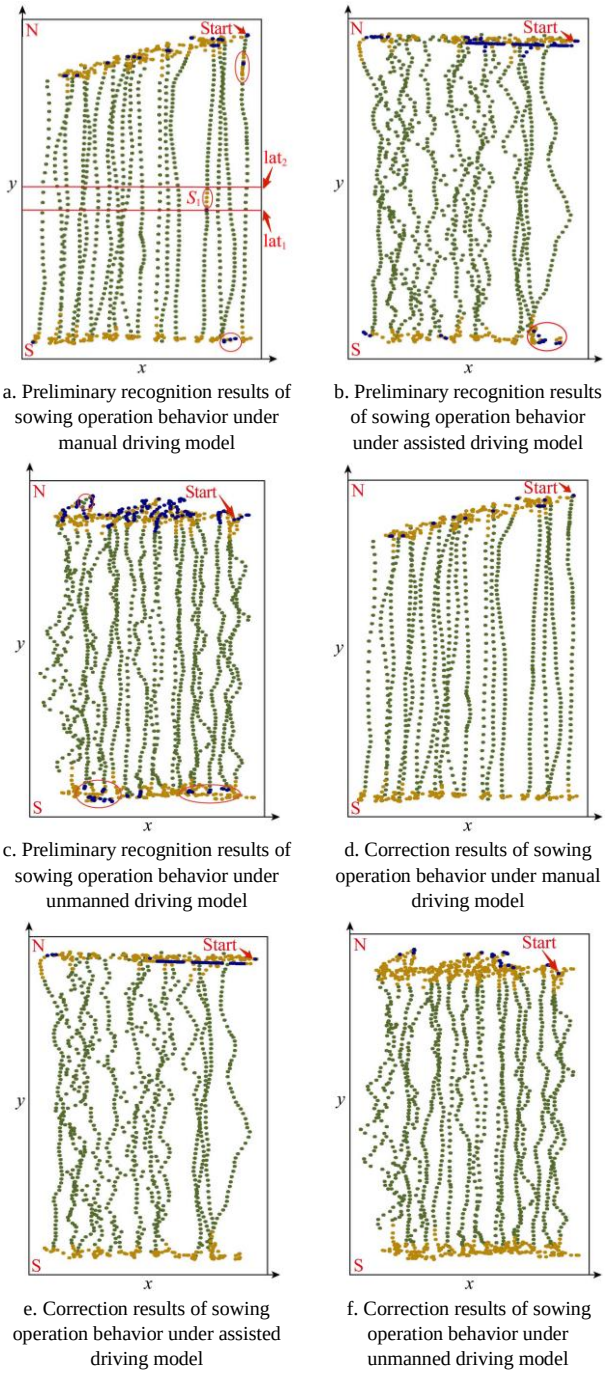

a. Preliminary recognition results of sowing operation behavior under manual driving model

b. Preliminary recognition results of sowing operation behavior under assisted driving model

c. Preliminary recognition results of sowing operation behavior under unmanned driving model

d. Correction results of sowing operation behavior under manual driving model

e. Correction results of sowing operation behavior under assisted driving model

f. Correction results of sowing operation behavior under unmanned driving model

Note: The green pointset represents the sowing behavior; the blue pointset represents the seed filling behavior; Yellow points are the turning behavior. The red circle denotes the error identification component. S_1 is the kinematical segment of error recognition, lat_1 and lat_2 are the latitude range of S_1.

Figure 3 Recognition results and correction results of the *K*-means algorithm

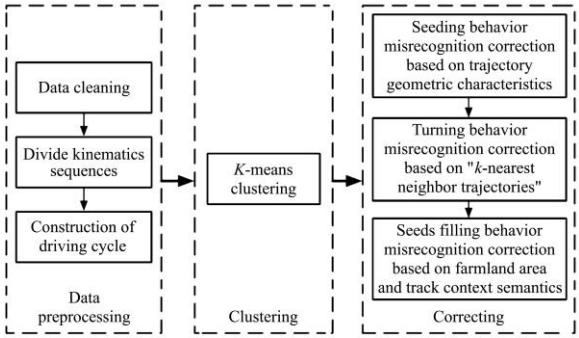

Figure 4 Roadmap of operation behavior recognition based on kinematic sequence semantic information

2.3.2 A correction algorithm for misidentified operating behavior

A three-step approach is described to adjust for three types of misidentifications in *K*-means clustering results: misrecognition of sowing behavior, misrecognition of turning behavior, and misrecognition of seeds filling behavior.

1) Sowing behavior misrecognition correction based on trajectory geometric characteristics (M1)

According to Table 4, there are 5.88% of Category 3 behavior is misdiagnosed as Category 1 behavior, and the corresponding trajectories are depicted by the green points set in the red circle in Figure 3c. The set of points has such geometric characteristics as a short length and a modest slope when the beginning points were connected with the endpoints in the trajectory sets. The characteristics are different from those of conventional tractor sowing. Define δ_1 as the shortest sowing distance, which is 50 m equal to the trial sowing distance[21]. Define δ_2 as the absolute value of the minimum slope at both ends of a set of continuous sowing trajectories. Given the possibility of a kinematic sequence with a steeper slope in Category 3, δ_2 is the upper quartile of the absolute value of the kinematic segment slope for Category 3, which is 13.19.

The steps of the misidentification correction algorithm for sowing behavior are as follows:

Step 1: Construct a sowing behavior continuous trajectories set $\boldsymbol{T_1}=\{T_1, T_2, T_3, \ldots, T_n\}$ where T_i is the i^{th} group of the continuous sowing trajectory. $\boldsymbol{T_i}=\{p_1, p_2, p_3, \ldots, p_n\}$, p_i is the i^{th} point.

Step 2: Calculate the length of each trajectory in $\boldsymbol{T_1}$, and construct the trajectory length set $\boldsymbol{D}=\{d_1, d_2, d_3, \ldots, d_n\}$, where d_i is the length of the connection line between two endpoints in $\boldsymbol{T_i}$. The absolute values of slope $\boldsymbol{T_i}$ are calculated round up to an integer, and the slope set $\boldsymbol{G}=\{g_1, g_2, g_3, \ldots, g_n\}$ is obtained.

Step 3: When d_i is less than δ_1 and g_i is less than δ_2, the label of T_i and the corresponding kinematic fragment are modified to 3.

2) Turning behavior misrecognition correction based on "*k*-nearest neighbor trajectories" (M2)

In Table 4, 5.88% of Category 1 behavior and 0.84% of Category 2 behavior were mistakenly identified as Category 3 behavior, and corresponding trajectories are displayed in the yellow points set in the red circle in Figure 3a. The trajectory points between the red lines are in the same latitude range as the wrongly identified kinematic segment S_1. The operation behaviors of adjacent trajectories are similar in the $[\text{lat}_1, \text{lat}_2]$ latitude range, and the closer the more similar the behavior is. Considering that Category 2 misidentification accounts for a very small proportion, this paper does not deal with it. A correction method of turning behavior misrecognition by "*K*-nearest neighbor trajectories" is proposed based on M1. The neighbor trajectories are defined as a set of continuous trajectory points, which have the same latitude as the kinematic sequence corresponding to Category 3 (example S_1) select majority labels of *K* group nearest neighbor trajectory points as "voting label". When "voting label" is not Label 3, Category 3 (example S_1) and its corresponding trajectory points label are modified to "voting label".

The selection of the *K* value is particularly important. When the *K* value is small, the different rate of the neighbor trajectories is small (the difference rate is equal to the number of minority labels), but it may not be able to obtain sufficient votes and affect the voting results. However, when the *K* value is too large, the different rates of neighbor trajectories themselves may increase, and the amount of data will also increase with the increase of the *K* value, increasing the running time of the algorithm. In order to determine the optimal *K* value of the three driving modes, the turning behavior was randomly sampled in an equal proportion in the three driving modes. The total number of samples is seventy-five kinematic sequences, accounting for 1/3 of all turning sequences. Calculate the relationship among the *K* value, the difference rate median, and the minimum votes of the *K*-nearest neighbor trajectories sample, Figure 5 shows the outcome.

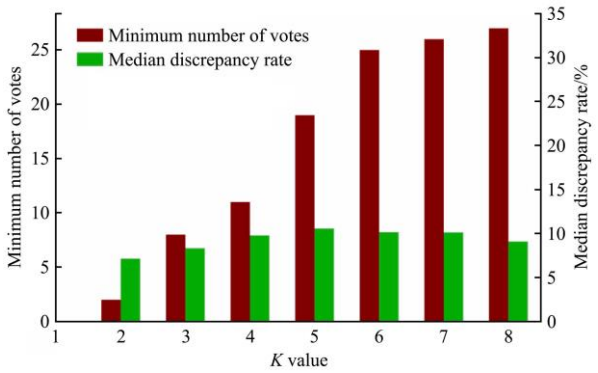

Figure 5 Relationship between the *K* value, the median difference rate, and the minimum number of votes

When *K*=1, the median difference rate is the minimum of 0, and the minimum votes are 0. When *K*=6, the median difference rate is 10.56%, and the minimum vote is 25. When *K*>6, with the increase of the *K* value, the median difference rate tends to be moderate, and the minimum votes increase slightly and tend to be stable. It can be assumed that the solution with the fewest votes collected at the time is the best solution, which means that the total votes for the *K*-nearest neighbor trajectories must be at least 25. The following steps are taken to correct the turning behavior error recognition:

Step 1: Using these data sets of the trajectory points and kinematic sequences after sowing correction, a kinematic sequence set $\mathbf{TS}=\{S_1, S_2, \ldots, S_n\}$ of turning behavior can be constructed. Where $\boldsymbol{S_i}$ is the i^{th} kinematic sequence, $\boldsymbol{S_i}=\{p_1, p_2, \ldots, p_n\}$, where p_i is the i^{th} point.

Step 2: Construct the neighbor trajectories set $\mathbf{NT}_i=\{T_1, T_2, \ldots, T_n\}$ of S_i, where T_i is the i^{th} neighbor trajectories, $\boldsymbol{T_i}=\{p_1, p_2, \ldots, p_n\}$ p_i is the i^{th} point on a trajectory, and sort the trajectories in NT_i according to the distance to S_i in ascending, the distance value to S_i is defined as:

$$\text{dis}=\sqrt{(x_i-\acute{x})^2+(y_i-\acute{y})^2} \tag{1}$$

where, (x_i, y_i) are central coordinates of T_i, and $(\acute{x}, \acute{y})$ are central coordinates of S_i.

Step 3: Select *K* groups of neighbor trajectories (*K* is 1 initially). If the total number of votes is fewer than 25, the *K* value is increased by 1. Calculate the ratio of label 1 points and label 3 points in the *K* groups of adjacent trajectories. If the ratio is not 1, the largest proportion label will be used as the "voting label". If the current S_i label is not equal to the "voting label", then modify the labels of the S_i and all points on S_i to the "voting label", otherwise, do nothing.

3) Misrecognition correction of seeds filling behavior based on farmland area and track context semantics (M3)

In Table 4, 5.88% of Category 1 behaviors and 81.51% of Category 3 behaviors were misidentified as Category 2 behaviors, and the corresponding trajectories are displayed in the blue points set in the red circle in Figures 3a and 3b. The blue points in Figures 3a and 3b are the seeds filling trajectories identified by the

clustering algorithm, which are distributed both in strip areas and turning areas. In this experiment, the seeds filling behavior happens only in the same direction of fields. Except for the first seeds filling operation, there will be turning behaviors before and after the seeds filling behaviors. Therefore, it is considered that the seeds filling behavior outlined by the red circle in the figure is a misidentification and needs to be corrected.

The steps of the seeds filling behavior misrecognition correction algorithm are as follows:

Step 1: Using these data sets of the trajectory points and kinematic sequences after turning correction, a continuous track set $\boldsymbol{T_2}$={T_1, T_2, …, T_n} of sowing behaviors can be constructed, where $\boldsymbol{T_i}$ is the i^{th} group seeds filling behavior trajectory, $\boldsymbol{T_1}$ represents the first seeds filling behavior trajectory, $\boldsymbol{T_i}$={p_1, p_2, …, p_n}, p_i is the i^{th} point. When the labels of the adjacent kinematic sequence to $\boldsymbol{T_i}$ are 1, the labels of $\boldsymbol{T_i}$ and the corresponding points on the kinematic sequence $\boldsymbol{T_i}$ are modified to 1.

Step 2: According to the timestamps of the start and end points the duration of $\boldsymbol{T_i}$ can be calculated. The duration of the seeds filling is not less than 60 s in general. Therefore, when both $\boldsymbol{T_i}$ and $\boldsymbol{T_1}$ are pointing in the same direction of the field, but the duration is less than 60 s, or when $\boldsymbol{T_i}$ and $\boldsymbol{T_1}$ are pointing in different directions, the labels of $\boldsymbol{T_i}$ and the corresponding points on the kinematic sequence $\boldsymbol{T_i}$ are modified to 3.

2.4 Fuel consumption forecast

In recent years, machine learning has become a high-quality solution to various regression problems[22-26]. In this study, principal component analysis and random forest algorithms are employed for current fuel consumption prediction. Compared with traditional fuel consumption prediction models, it avoids the need to master the knowledge of the internal structure of the vehicle and the principle of the engine. On the basis of the feature matrix $\boldsymbol{A}$ of the tractor driving cycle, the feature matrix $\boldsymbol{B}$ of the fuel consumption prediction model is constructed by adding the operation behavior characteristic X_1 and the driving mode characteristic X_2, $\boldsymbol{B}=[\bar{V},V_{std},...,X_2]$. This study performs principal component analysis on feature matrix $\boldsymbol{B}$ to reduce the dimension of the feature matrix and eliminate the collinearity between features. The contribution rate of the cumulative variance of the principal components is listed in Table 5. As can be observed, the cumulative variance contribution rate of the first three principal components reaches 86.38%. Additionally, the eigenvalues exceed 1 and the variance contribution rate is high, indicating that the first three principal components capture the majority of the information contained in the original characteristic data.

Table 5 Feature matrix *B* principal component cumulative variance contribution rate

Principal component	Eigenvalues	Variance contribution rate/%	Cumulative contribution rate/%
Z_1	3.258	40.724	40.724
Z_2	2.646	33.081	73.805
Z_3	1.006	12.571	86.376
Z_4	0.610	7.621	93.997
Z_5	0.226	2.827	96.824
Z_6	0.149	1.863	98.687
Z_7	0.105	1.313	100
Z_8	-1.72×10^{-14}	-2.15×10^{-13}	100

Loads of the original features in the first three principal components Z_1, Z_2, and Z_3 are listed in Table 6. The principal component load data reflects the correlation between the principal component and various characteristics. The greater the absolute value of the load data, the more the principal component can reflect the characteristics[27]. As can be seen from Table 6, the principal components Z_1, Z_2, and Z_3 contain the information contained in the original eight characteristic parameters. Z_1 mainly includes $\bar{V}$, $P_{\bar{V}}$, P_C, X_1. Z_2 mainly includes V_{std}, P_a+, P_a–. Z_3 mainly includes X_2. This study selects the scores of the first three principal components to construct the feature matrix $\boldsymbol{C}$ of the fuel consumption prediction model, $\boldsymbol{C}$=[Z_1, Z_2, Z_3].

Table 6 Principal components Z_1, Z_2, and Z_3 load information

Original features	Z_1	Z_2	Z_3
$\bar{V}$	0.51	0.16	−0.13
V_{std}	−0.05	0.57	0.06
P_a+	−0.11	0.47	0.07
P_a–	−0.11	0.48	−0.11
$P_{\bar{V}}$	0.53	0.12	0.02
P_C	−0.49	−0.26	−0.02
X_1	−0.43	0.33	0.11
X_2	−0.10	0.04	−0.97

Note: $\bar{V}$ is the value of the average working speed of the tractor; V_{std} is the speed standard deviation; P_a+ is the acceleration time ratio; P_a– is the deceleration time ratio; $P_{\bar{V}}$ is the uniform time ratio; P_C is the idle time ratio; X_1 is the operation behavior characteristic; X_2 is the driving mode characteristic; Z_1, Z_2, and Z_3 are the first three principal components of the feature matrix $\boldsymbol{B}$.

This study divides the 1139 data of the feature matrix $\boldsymbol{C}$ into 910 training samples and 229 test samples at the ratio of 8:2. The number of decision trees in the random forest has the biggest impact on the accuracy of fuel consumption prediction. Few decision trees will lead to lower model prediction accuracy, and too many decision trees will increase the training time sharply. The relationship between the number of decision trees and the model average error and the training duration is demonstrated in Figure 6.

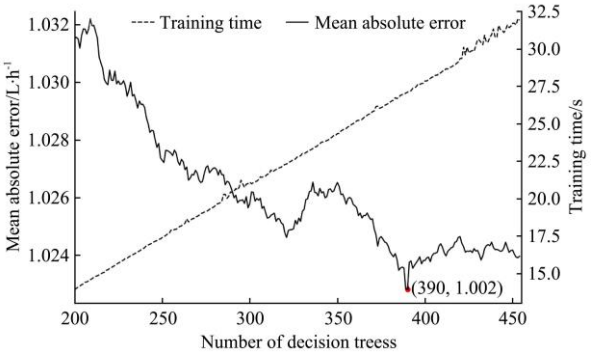

Figure 6 Relationship between the number of decision trees, the mean absolute error, and the training time

As illustrated in Figure 6, the average absolute error of fuel consumption prediction decreases steadily as the number of decision trees rises, while training time increases consistently. When the number of decision trees reaches 390, the average absolute error of the model on the validation set reaches the minimum value. In order to avoid overfitting, the depth h of the decision tree, the minimum number of samples n required for node splitting, and the minimum number of samples m contained in each leaf node are limited. Additionally, to confirm the prediction model's accuracy and stability, 10-fold cross-validation is performed on the training set. Using the grid search method, it is implied that when h=9, n=2, and m=2, the average absolute error of the fuel consumption prediction model on the validation set is at

least 0.997 L/h.

3 Results and analysis

3.1 Evaluation of operation behavior recognition algorithms

The corrected *K*-means recognition results for the three driving modes are shown in Figures 3d-3f. Three evaluation indicators of Precision, Recall, and F1 score were used to evaluate the operation behavior recognition algorithm based on the semantic information of the kinematic sequence. The evaluation indicators are calculated as follows:

$$\text{Precision} = \frac{\text{TP}}{\text{TP} + \text{FP}} \tag{2}$$

$$\text{Recall} = \frac{\text{TP}}{\text{TP} + \text{FN}} \tag{3}$$

$$\text{F1 score} = \frac{2\ \text{Precision} \times \text{Recall}}{\text{Precision} + \text{Recall}} \tag{4}$$

where, Precision is the accuracy of a certain kind of operation behavior recognition; Recall is how much of a certain kind of operation behavior is recognized correctly; F1 score is the harmonic mean of precision and recall. The method proposed in this study and the *K*-means algorithm were separately used to identify 1139 kinematic sequences. The comparison results are listed in Table 7. The F1 score for recognizing sowing behavior increased by 2.06%, that for recognizing seeds filling behavior increased by 8.99%, and that for recognizing turning behavior increased by 21.79%. The method proposed in this study had higher recognition accuracy for the operation behavior of the three driving modes.

Table 7 Behavior recognition algorithm evaluation

Driving mode	Method	Sowing			Seeds filling			Turning		
		Precision	Recall	F1 score	Precision	Recall	F1 score	Precision	Recall	F1 score
Manual	*K*-means	1.00	0.92	0.96	0.93	0.99	0.96	0.92	0.89	0.90
	K-means+M1+M2+M3	1.00	0.99	0.99	1.00	0.97	0.99	0.92	1.00	0.96
Assisted	*K*-means	0.96	1.00	0.98	0.81	1.00	0.90	1.00	0.65	0.79
	K-means+M1+M2+M3	0.98	1.00	0.99	0.94	1.00	0.97	0.94	0.96	0.97
Unmanned	K-means	0.98	0.98	0.98	0.67	1.00	0.80	0.98	0.54	0.70
	K-means+M1+M2+M3	1.00	0.98	0.99	0.90	1.00	0.95	0.98	0.90	0.94
Total	*K*-means	0.98	0.97	0.97	0.80	1.00	0.89	0.96	0.65	0.78
	K-means+M1+M2+M3	0.99	0.99	0.99	0.96	0.98	0.97	0.95	0.94	0.95

Note: Precision is the accuracy of a certain kind of operation behavior recognition; Recall is how much of a certain kind of operation behavior is recognized correctly; F1 score is the harmonic mean of precision and recall; "Total" represents the comprehensive performance of the model under three driving modes.

3.2 Tractor fuel consumption analysis

To investigate the variations in fuel consumption between tractor operating modes and operating behaviors, the instantaneous power, and instantaneous fuel consumption were calculated for three operating behaviors. Due to the fact that the seeds filling behavior is present with a long time standing still in all driving modes, this study will focus on an investigation of the sowing and turning behaviors. The power calculation equation is shown in Equation (5)[28]:

$$p_i = \frac{r_i \times t_i}{9545.45} \tag{5}$$

where, r_i is the rotation speed in the i^{th} s, r/min; t_i is the torque in the i^{th} s, N·m; p_i is the power in the i^{th} second, kW; 9545.45 is a constant.

Table 8 lists the average power of the tractor as sowing time arrange from high to low as manual driving, unmanned driving, and assisted driving. Average instantaneous fuel consumption has the same rule. The average tractor power as turning time arrange from high to low as unmanned driving, manual driving, and assisted driving. The average instantaneous fuel consumption of a single turning has the same rule. These conform to the positive correlation between power and fuel consumption. Overall, the assisted driving mode has the lowest fuel usage for both sowing and turning behavior. The three indicators are comparable in terms of the number of starts and stops, the average duration of a single turning, and average instantaneous fuel consumption of a single turning since the turnings in the manual driving mode and the assisted driving mode are all manual activities, the turning route is demonstrated in Figure 1a and Figure 1b by drawing lines in the turning area. But the average instantaneous fuel consumption of manual driving is slightly higher than that of auxiliary driving. That is consistent with the two average turning power. In unmanned mode, the software controls the turning, the turning route is demonstrated in Figure 1c with the line drawn in the turning area and there are several starts and pauses, which may account for the increased average instantaneous fuel consumption of a single turn.

Table 8 Sowing behavior and turning behavior of three driving modes working condition statistics

Driving mode		Manual	Assisted	Unmanned
Sowing behavior	Average speed/m s^{-1}	2.71	2.20	1.57
	Average power/kW	69.37	51.21	56.62
	Average instantaneous FC/L h^{-1}	17.44	13.11	15.98
Turning behavior	Average speed/m s^{-1}	0.65	0.57	0.29
	Average power/kW	23.37	20.09	27.49
	Start and stop times/times	8	8	13
	Average time for a single turn/min	1.05	1.30	2.09
	Average instantaneous FC for a single turning/L h^{-1}	5.89	5.51	7.62

Note: FC is fuel consumption.

The investigation demonstrates that fuel usage is affected by both operating behavior and driving mode. In this study, three operating behaviors and three driving modes are mapped to numbers 0, 1, and 2 as the contributing elements of the fuel consumption prediction model.

The manual driving mode's operation is completely manual, from sowing to turning, and the sowing and turning speeds are both high, resulting in the highest possible work efficiency. The assisted driving mode operation saves time and labor during sowing operations and has nothing to do with the agricultural machine operator's driving ability. The turning efficiency of assisted driving mode operation is comparable to that of manual

work, and the work efficiency is higher. From sowing to turning around, the unmanned mode of operation is completely unmanned. However, due to the performance of tractor hardware (such as electronically controlled steering wheels) and personnel safety, the speed of driving and turning in the field is limited, resulting in low overall work efficiency. The average instantaneous fuel consumption of the three driving modes is compared. In manual driving mode, the speed is manually controlled for sowing and turning, and there are other gears and speeds available. High gears and high speeds lead to higher vehicle power and maximum fuel consumption. Sowing and turning safety are manually regulated in assisted driving mode, which can intelligently raise gear and speed, reduce vehicle power, and minimize fuel consumption. In the unmanned driving mode, a low-speed operation is used to manage the sowing quality and turning, and the engine torque and the vehicle power both increase, resulting in higher fuel consumption. By calculating the average lateral error of the sowing track and the average error of the sowing trajectory spacing, the manual driving mode had considerable speed and direction variations. The average lateral error of a sowing trajectory is 0.120 m, whereas the average spacing error of a sowing track is 2.494 m. The assisted driving mode has a considerable speed fluctuation but a minor direction fluctuation; the average lateral error of the trajectory is 0.087 m, while the average error of the sowing trajectory spacing is 1.786 m. The fluctuations in speed and direction of the unmanned driving mode are small, the average lateral error of the trajectory is 0.041 m, and the average error of the spacing between the sowing tracks is 0.497 m. For maize sowing, the assisted driving mode is the optimal mode of operation, in terms of efficiency, fuel consumption, and operating quality. In this study, 6 driving cycle indicators, three operating behaviors, and three driving modes were selected to construct the feature matrix of fuel consumption prediction, and a model for tractor sowing fuel consumption prediction was constructed using the principal component analysis and random forest algorithms. The relative error of model prediction under three driving modes is 0.11 L/h, reliable predictions can be made for agricultural machinery maize sowing fuel consumption. After the fuel consumption prediction model is established, smartphone data can be directly used for agricultural fuel consumption detection, which changes the traditional fuel consumption collection method and saves equipment installation costs. The behavior recognition and fuel consumption prediction model of tractor sowing operations based on smartphone positioning data can provide a convenient operation evaluation and supervision for operators and farmers.

3.3 Evaluation of fuel consumption prediction model of agricultural machinery

The relationship between the predicted value of the fuel consumption prediction model and the actual value is demonstrated in Figure 7.

As can be seen, the predicted values are essentially dispersed on either side of the actual fuel consumption and extremely approximate to it. The model has a high degree of fitness. The average absolute error (MAE), determination coefficient R2 and average relative error K are used to evaluate the accuracy of the fuel consumption prediction model. The calculation equations are as follows:

$$\mathrm{MAE}=\frac{1}{n}\sum_{i=1}^{n}|\hat{y}_i-y_i| \tag{6}$$

$$R^2=1-\frac{\sum_{i=1}^{n}(y_i-\hat{y}_i)^2}{\sum_{i=1}^{n}(y_i-\bar{y})^2} \tag{7}$$

$$K=\frac{1}{n}\sum_{i=1}^{n}\frac{|y_i-\hat{y}_i|}{y_i} \tag{8}$$

where, $\hat{y}_i$ is the i^{th} predicted fuel consumption value in the test set, L/h; y_i is the i^{th} actual fuel consumption value in the test set, L/h; n is the number of samples in the test set; $\bar{y}$ is the average value of real fuel consumption in the test set, L/h.

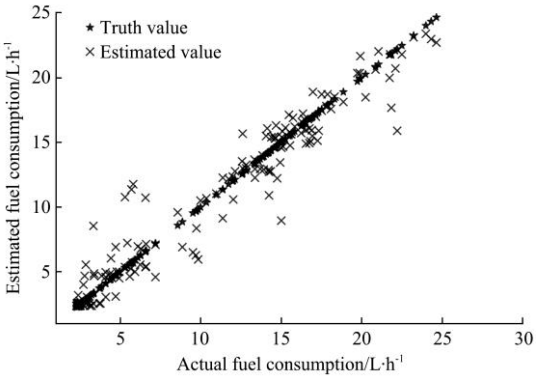

Figure 7 Relationship between predicted fuel consumption and actual fuel consumption

The evaluation results are shown in Table 9. The prediction model can reasonably predict the fuel consumption of agricultural machinery for sowing. The average relative error and average absolute error of the fuel consumption prediction model in the manual driving mode are the lowest. The speed variances of manual driving, assisted driving, and unmanned driving are 1.78 m/s, 1.11 m/s, and 0.58 m/s, respectively. In comparison to the other two driving modes, manual driving is less stable in terms of speed control and has the highest variance in vehicle speed. In addition, the driving cycle characteristics of manual driving contain more information, resulting in the best prediction model fitting effect.

Table 9 Evaluation of fuel consumption prediction models

Driving mode	MAE/L ħ$^{-1}$	R^2	K/L ħ$^{-1}$
Manual	0.61	0.98	0.09
Assisted	0.83	0.95	0.10
Unmanned	1.19	0.91	0.14
“Total”	0.90	0.95	0.11

Note: “Total” represents the comprehensive performance of the model under three driving modes. MAE means the average absolute error.

4 Conclusions

In this study, three modes of driving: manual, assisted, and unmanned are presented and discussed in maize sowing operations. By dividing trajectory points into several kinematic sequences based on time windows, the driving cycle index of the kinematic sequence is constructed, which compresses the amount of data while providing more semantic information for a single point. Based on the semantic information of the tractor kinematics sequence, this paper proposes a behavior recognition method for sowing operations of the tractor. After K-means clustering, three correction schemes are proposed to finish the behavior of the operation identified:

1) Sowing behavior misrecognition correction based on trajectory geometric characteristics;

2) Turning behavior misrecognition correction based on "*k*-nearest neighbor trajectories";

3) Seeds filling behavior misrecognition correction based on farmland area and track context semantics;

Compared with the *K*-means algorithm, the F1 score is improved by 2.06%, 8.99%, and 21.79% in sowing behavior recognition, seeds filling behavior recognition, and turning behavior recognition respectively. The weighted average F1 score of the method proposed in this study reached 0.96 in all three driving modes, suggesting that it is capable of accurately identifying operation behaviors. It offers the groundwork for analyzing the tractor's fuel use. There are still a few misidentifications that are not corrected. The potential reason is that the multiple thresholds in the correction algorithm are needed to adjust.

This study proposed a method for behavior recognition and predicting fuel consumption of agricultural machinery sowing behavior based on smartphone positioning data. The positioning data was collected by smartphone, which is more convenient than fixed GNSS equipment and OBD equipment. However, there are some limitations in the current study that are worth highlighting. First of all, the farmland in this experiment is large and regular in shape, but it is unavoidable for agricultural machinery to operate in a small area of farmland. Therefore, more data are needed to support the proposed method. Secondly, different crops have different requirements for sowing depth and soil moisture. At present, this study is only for maize sowing, so there may be inevitable deviations in the results of the fuel consumption prediction method proposed in this study for sowing other crops. In the future, data on various types of operations of more types of agricultural machinery will be collected in irregular farmland. Expanding the data set, enriching the feature input of the model, and improving the universality of the model will be the next phase of work.

Acknowledgements

The authors acknowledge that this work was financially supported by the Research and Integrated Demonstration of Technologies of Autonomous operation for Agricultural Vehicle Unmanned Driving of Beijing Municipal Science and Technology Commission (Grant No. Z201100008020008).

[References]

[1] Qu Y L. Impact of fuel oil on the operating cost of agricultural machinery should not be underestimated. Agriculture Machinery Technology Extension, 2014; 12: 42–43. (in Chinese)

[2] Xiao H, Relationship between the concept of green agriculture and the development of agricultural mechanization and its combined advantages. Agricultural Machinery Using & Maintenance, 2020; 6: 41. (in Chinese)

[3] Barth M, An F, Younglove T, Levine C, Scora G. Development of a comprehensive modal emissions model. Transportation Rsearch Board, 2000; 435p.

[4] Cheng Y, Zhang J L, Zhang S J, Guo J F, Zhang D. Evaluation of eco-driving behavior and fuel-saving potential of large freight vehicles. Journal of Transportation Systems Engineering and Information Technology, 2020; 20(6): 253–258. (in Chinese)

[5] Gu Q H, Wang Q, Jiang S, Ma P P. Research on fuel consumption prediction of truck in open-pit mine based on PSOGA-SVM. Mining Research and Development, 2021; 41(8): 161–166. (in Chinese)

[6] Sun R X, Chen Y H, Dubey A, Pugliese P. Hybrid electric buses fuel consumption prediction based on real-world driving data. Transportation Research: Part D: Transport and Environment, 2020; 91: 102637. doi: 10.1016/j.trd.2020.102637.

[7] Perrotta F, Parry T, Neves L. Application of machine learning for fuel consumption modelling of trucks. 2017 IEEE International Conference on Big Data (Big Data), Boston, USA, 2017; pp.3810–3815. doi: 10.1109/BigData.2017.8258382.

[8] Yao Y, Zhao X H, Zhang Y L, Chen C, Rong J. Modeling of individual vehicle safety and fuel consumption under comprehensive external conditions. Transportation Research Part D: Transport and Environment, 2020; 79: 102224. doi: 10.1016/j.trd.2020.102224.

[9] Li X. Effective measures for prevention and control of agricultural machinery pollution. Fujian Agricultural Machinery, 2020; 2: 6–9. (in Chinese)

[10] Zhao B D, Feng L L, Deng Y, Cao L H. Real-time online compression method for vehicle trajectory based on smart phone sensors. Journal of Southwest Jiaotong University, 2022; 57(1): 1–10. (in Chinese)

[11] Hu S, Wu Z C, Zhang J. Driving behavior recognition based on data depth features of vehicle mobile phone. Computer Applications and Software, 2019; 36(1): 59–66, 87. (in Chinese)

[12] Yang J D, Cao Y C, Lin Q, Man Z X, Liu X S. Research on traffic status recognition based on mobile phone sensors. Journal of Northwest Minzu University (Natural Science), 2019; 40(4): 1–8. (in Chinese)

[13] Kou Z H. A method of agricultural machinery operation perception and behavior modeling based on smartphone sensors. Master's dissertation. Beijing: China Agricultural University, 2018; 44p. (in Chinese)

[14] Kong Q H, Maimaiti T, Zhao M J. Recognition of tractor working condition based on convolutional neural network. Journal of Chinese Agricultural Mechanization, 2021; 42(11): 144–150. (in Chinese)

[15] Zou B, Shi Z X, Du S H. Gases emissions estimation and analysis by using carbon dioxide balance method in natural-ventilated dairy cow barns. Int J Agric & Biol Eng, 2020; 13(2): 41–47.

[16] GB/T 38146.2-2019. Vehicle driving conditions in China - Part II: Heavy commercial vehicles. (in Chines)

[17] Castano F, Rossi A, Sevaux M, Velasco N. A column generation approach to extend lifetime in wireless sensor networks with coverage and connectivity constraints. Computers & Operations Research, 2014; 52(Part B): 220–230.

[18] Huang Z F, Xue J, Ming B, Wang K R, Xie R Z, Hou P, et al. Analysis of factors affecting the impurity rate of mechanically-harvested maize grain in China, Int J Agric & Biol Eng, 2020; 13(5): 17–22.

[19] Jia T L. AF-Verifying theorem deduced from two factors distribution. Journal of Southwest University of Science and Technology, 2004; 19(3): 89–91, 97. (in Chinese)

[20] Chen Y, Zhang X Q, Wu C C, Li G Y. Field-road trajectory segmentation for agricultural machinery based on direction distribution. Computers and Electronics in Agriculture, 2021; 186: 106180. doi: 10.1016/j.compag.2021.106180.

[21] Li C Y. Analysis of technical requirements and implementation misunderstandings of maize mechanized sowing operations. Agricultural Machinery Using & Maintenance, 2021; 12: 26–27. (in Chinese)

[22] Ye Q P, Yu S C, Liu J L, Zhao Q X, Zhao Z. Aboveground biomass estimation of black locust planted forests with aspect variable using machine learning regression algorithms. Ecological Indicators, 2021; 129: 107948. doi: 10.1016/j.ecolind.2021.107948.

[23] Bu J H, Tian Y X, Zong Y F. Analysis on the influencing factors of multiple indicators in the United States based on multiple linear regression model. Journal of Physics: Conference series, 2021; 1952(4): 42083. doi: 10.1088/1742-6596/1952/4/042083.

[24] Yuan F Q, Liu J M. Anomaly detection for environmental data using machine learning regression. IOP Conference Series. Materials Science and Engineering, 2019; 472(1): 12089. doi: 10.1088/1757-899X/472/1/012089.

[25] Kr. Jha S, Ahmad Z. Soil microbial dynamics prediction using machine learning regression Methods, Computers and Electronics in Agriculture, 2018, 147: 158–165.

[26] Fu Q, Shen W Z, Wei X L, Yin Y L, Zheng P, Zhang Y G, et al. Predicting the excretion of feces, urine and nitrogen using Support Vector Regression: A case study with holstein dry cows. Int J Agric & Biol Eng, 2020; 13(2): 48–56.

[27] Yun S K, Kim J, Im E S, Kang G C. Behavior of porewater pressures in an earth dam by principal component analysis. Water, 2022; 14(4): 672. doi: 10.3390/w14040672.

[28] Zhou L B. Internal combustion engine. Beijing: Machinery Industry Press, 1990; 352p. (in Chinese)